THE DESIGN, ASSEMBLY AND PERFORMANCE OF THE SIN BEAM TRANSFER LINE

Ch. Markovits, L. Rezzonico, J. Zichy

Schweizerisches Institut für Nuklearforschung (SIN), 5234 Villigen, Switzerland

Abstract

The beam line between the Philips isochronous cyclotron (injector) and the ring accelerator was put into operation in November 1973. The basic features of this beam line are described.During the last year the transmission of the beam was successively improved. The control of the beam was facilitated by the excellent performance of the beam diagnostic elements. Some results are presented on beam measurements which show the performance of the transfer line.

1. Design criteria

As soon as the concept of the two stage acceleration had been invented, we started to consider the design of the beam transfer line. The main requirements were:

a) The horizontal and vertical phase areas of the injector should be measurable and restrictable.

b) The energy width of the beam should be restricted to $\leq$ 100 keV FWHM.

c) The phase areas and the energy of the beam should be matched to the acceptance of the ring accelerator.

d) No quadrupole should be placed inside the ring accelerator.

e) There must be a 2 m long beam blocker in the beam transfer line.

Once the definite choice of the injector had been made, we could very soon specify the necessary floor layout. By then, the size of the experimental hall had already been fixed. In order to maximise the area used for physics, we had to make some sacrifice on the optimal layout of the transfer line, with the following consequences:

a) The beam matching and the beam measuring section of the transfer line are not separated.

b) We had to choose a "Z"-shaped beamline, which results in larger horizontal amplitudes than a "U"-shaped one.

The final floor layout is shown in fig. 1.

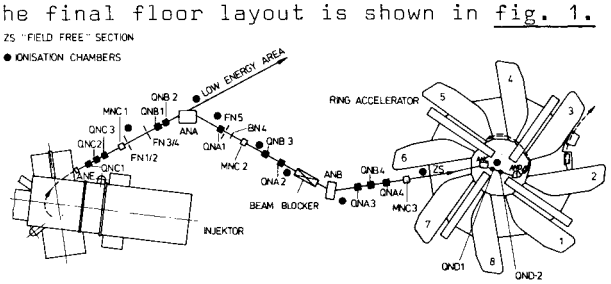

Fig. 1: The final layout of the transfer line.

The horizontal and vertical phase areas of the beam were guaranteed by N.V. Philips Eindhoven to be smaller then 30 mm mrad. Their design goal was the delivery of an almost achromatic beam.

2. Optical properties

Throughout this paper we call the dispersion path the path of a particle with a momentum 1 per mil larger than the mean momentum and which is at the centre of the corresponding phase area. Such particles have to be injected at a larger radius of the ring accelerator than the particles with the mean momentum. The quality of the incoming beam is measured in the first part of the beam transfer line. The injector was delivered with a large angle horizontal steering magnet ($\pm$ 2,5° = ANE) and with a triplet (QNC1, QNC2 and QNC3). These lenses enable us to focus the beam in both transverse planes. The two waists must be separated in order to avoid damage to the monitors. The horizontal waist serves as source for the subsequent low resolution analysing system. The analysis is done by a 57° bending magnet (ANA) and a doublet (QNB1, QNB2) in front of it. Behind the 57° bending magnet is a single lens (QNA1), which enables us to move the image to the right position. The next part of the beam line matches the beam to the acceptance requirements of the ring accelerator. To decrease the energy resolution of the beam behind the dispersive image of the analysing system we must have a crossover of the dispersion path before the beam enters the -37° bending magnet (ANB). The crossover is produced by the next quadrupole (QNB3). The following lens (QNA2) is needed to maintain small vertical amplitudes in the -37° bending magnet. With the three lenses (QNA3, QNB4 and QNA4) behind this magnet we have to match the beam to the proper phase areas at injection into the ring accelerator. Behind these lenses the beam crosses radially a "field free"-section (ZS) of the ring accelerator, where it is slightly (-3 °) bent. Inside the ring accelerator there are three large angle bending magnets (ANC = 30°, AND1 = -50°, AND2 = -50°) which are used to guide the beam to injection. The first -50° bending magnet has a vertically focussing entrance edge. Behind the -37° bending magnet the dispersion path has two further crossovers. The first one lies in the first lens (QNA3) of the triplet, the next one in the first -50° bending magnet (AND1).

Three lenses of the transferline are placed in such a way that the independent tuning of the vertical and horizontal phase areas at

Proc. 7th Int. Conf. on Cyclotrons and their Applications (Birkhäuser, Basel, 1975), p. 306-311

injection should be feasible[1]. As may be seen in fig. 2, the crossovers occur inside the quadrupoles QNA2 and QNA3, and thus there are horizontal waists near these elements. A vertical waist is located inside the quadrupole QNB4. By making small changes in the excitations of these lenses, it is possible to change the phase area in only one plane.

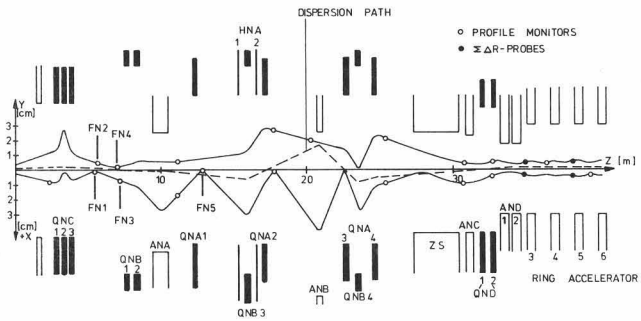

Fig. 2: The horizontal and vertical beam envelopes and the arrangement of the monitors. The dispersion path is only sketched, the envelopes are calculated.

After some weeks of beam production we realised that in order to make fine tuning easier, it would be preferable to place two small lenses (QND1 and QND2) inside the ring accelerator, i.e. we had to drop one of our design criteria. This is because the triplet which is used for the beam matching is more than 10 meters away from the injection into the ring accelerator.

To provide active second order corrections, two sextupoles (HNA1 and HNA2) are placed between the dispersive image and the -37° bending magnet. As a further second order correction the entrance- and exit-edges of this magnet have a fixed curvature. The position and strength of the second order correction elements were recommended by H.A. Enge[2].

3. Assembly of the transfer line

The greater part of the beam guiding magnets were fabricated by SCANDITRONIX AB. The three bending magnets inside the ring accelerator were designed by SIN and manufactured by different firms in the USA. The additional quadrupoles inside the ring accelerator, the ± 2.5° horizontal steering magnet together with the first triplet were purchased from N.V. Philips Eindhoven.

The different beam monitors, all the mechanical support, the vacuum system and the necessary electronics were designed by and, in their bulk, manufactured at SIN. The monitors are mounted into standard cubes, called measuring boxes, at most four in one box. All the beam guiding elements and the measuring boxes are aligned with respect to rigid iron bars,except those inside the ring accelerator. This makes realignment faster if the foundations move. The accuracy of the alignment is better than ± 0.3 mm. The whole transfer line is divided into five vacuum sections separated by valves. The vacua in the injector and ring accelerator extend into the first and last sections respectively.

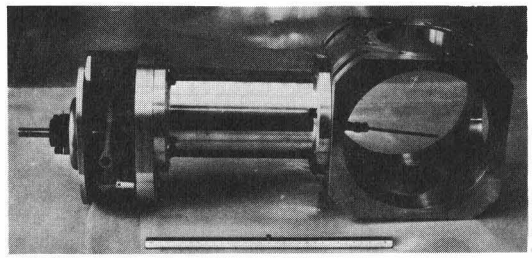

Fig. 3: The profile monitor in a measuring box.

The whole vacuum system, except in the bending magnets, is made out of aluminium to guarantee a short cooling down period in case of beam losses. The vacuum chambers of the bending magnets are made out of stainless steel. To evacuate the beamline, we use three turbomolecular pumps, each having its own backing pump. The resulting vacuum is better than 10^{-5} Torr. The pumping capacity is chosen in such a way that the failure of one pump has no serious effect on the pressure in the transfer line. We use only rubber seals in the vacuum system, and we expect to replace them every second year.

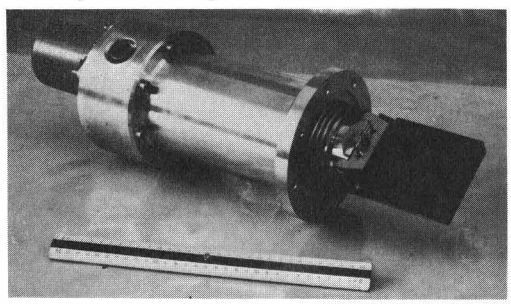

Fig. 4: One jaw of the slit

4. Beam steering

There are four horizontal and five vertical steering magnets in the transfer line. After emerging from the injector we center the beam in both planes. As a vertical steerer, we use the outermost concentric trim coil of the injector, excited assymetrically. Since this trim coil affects the extraction, it would have been preferable to have an additional vertical steerer immediately after the injector. In the transfer line we have vertical steerers only where two supporting iron bars join each other. The reason for this is that the components on the same supporting iron bars do not move with respect to each other. Before injecting into the ring accelerator we have an additional horizontal and vertical steerer in order to center the beam in its first turns. A steerer is also mounted in front of the -37° bending

magnet, for minimization of intensity losses in the magnet's vacuum chamber.

5. Beam monitoring

Adequate quality of the monitors and their proper positioning along the beam line are essential to achieve a satisfactory beam performance. The monitors have two purposes. First they allow continuous control of the beam during production runs, and secondly they measure the beam quality accurately.

5.1 The profile monitor (MNP) is shown in fig. 3. It swings a thin molybdenum finger through the beam[3]. This isolated finger is fastened to an arm, which is moved by a DC-motor eccentrically. The position of the finger with regard to the optical axis is registered by a linear potentiometer. The beam profile is given in one of the two possible planes by the current of the stopped protons, plus that of the knocked out secondary and δ-electrons. Thus the efficiency of the profile monitor lies between 120 % and 200 %. With this fast monitor (max. 3 swings/s) one may measure beam profiles of proton beams in the intensity range from 10 nA up to 100 µA. The profiles can be directly displayed on a storage scope.

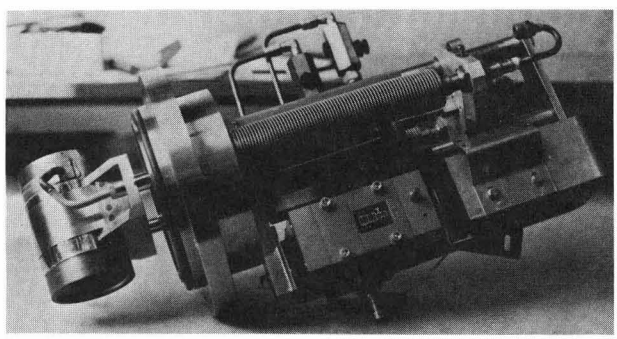

Fig. 5: The beam stopper

5.2 The slit (FN), one half of which is shown in fig. 4, is used for slow measurements of profiles and emittances. It is also suitable for limiting the beam emittance. The water cooled copper jaw, which can absorb up to 5 kW, is mounted on a spindle and driven by a stepping motor. A high precision potentiometer registers the slit position. The current of the stopped protons in each isolated jaw is measured by a picoammeter through an analog-multiplexer. The positioning of the jaws is accurate to 0.1 mm and the range of movement is 90 mm. The speed of the slit movement is not faster than 2 mm/s.

5.3 To measure the beam intensity we have two different types of monitors.

5.3.1 The beam stopper (BN) is essentially an isolated copper block, which one may move pneumatically into the beam to stop the protons (see fig. 5). This water cooled, round, copper block can absorb up to 8 kW beam power. On the upstream side of the beam stopper a conical hole is drilled into the copper block. This hole reduces the distributed power per unit surface area. The beam stopper is also used in the personnel safety system and in the machine control interlock system. To make a more precise current measurement we add a copper pipe to the beam stopper to make a simple Faraday cup. The copper pipe in front of the beam stopper, is isolated from the beam pipe and electrically connected to the copper block, it collects the knocked-out electrons.

5.3.2 The current transformer (MNC) is a non-intercepting current measuring monitor. It is essentially a coaxial resonator with a high Q-value[4]. The beam crosses it axially and excites it in a TM01-mode oscillation. The amplitude of this oscillation is proportional to the beam intensity. To have a low signal to noise ratio on the decoupled signal the resonator works on the second harmonic of the RF-frequency. The measuring range lies between 100 nA and 250 µA with about 1 % accuracy.

5.4 The ionisation chambers (MNI) are put beside the transfer line in strategic places and detect the beam losses in their vicinity. The air filled ionisation chambers have a volume of 2 l and have 6 high voltage plates besides 5 collecting plates (see fig. 6). The collected current is fed into a logarithmic current to voltage converter[5]. The converter range lies between 1nA and 1mA and its signal is displayed. With adjustable comparators we set two signal levels, the lower of which gives a warning, and the higher one is fed into the interlock system. The ionisation chamber signals beam losses greater than 100 nA.

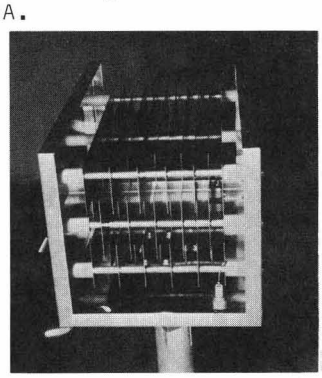

Fig. 6: The ionisation chamber

5.5 The center of gravity monitor (MNS) also a non-intercepting device has recently reached a satisfying working performance. The signal to noise ratio at the second harmonic of the RF-frequency is now large enough to operate it above 1 µA.

6. Beam performance

Since the first beam passed along the transfer line we have had no major failures resulting

in beam-time losses. The transfer line is capable of injecting the whole beam into the ring accelerator but usually we restrict it and lose up to 10 % of beam intensity. This is due to the varying energy width and emittance of the extracted beam.

Along the transfer line we distributed various monitors in such a manner that we can measure the incoming beam quality, the beam size at the waist positions and at places where the aperture of the elements is constricting. Three profile monitors are mounted at the inner radius of the ring accelerator too.

6.1 Incoming beam. In the straight section behind the first triplet we have waists in both transverse planes, where the slits FN1 and FN4 are mounted. In the same straight section are two other slits, FN3 and FN2 (see also figs. 1 and 2). In front of each slit is a corresponding profile monitor. At the image plane of the subsequent analysing system there is another slit (FN5) and a beam stopper (BN4). This system measures the quality of the incoming beam.

6.1.1 To make a fast but rough emittance measurement we use the profile monitors. We move the waist into the corresponding profile monitor and determine the beam size on the corresponding monitors. In a similar way we may use two slits, closing them until the intensity loss amounts to a certain percentage of the total intensity. A very nice measuring method makes use of the slit FN1 in the waist and the profile monitor MNP3 downstream. We make a small slit opening and by moving this window stepwise across the waist we can scan the transmitted beam at each step with the profile monitor. The result of this measurement may be directly displayed on a storage scope as a phase ellipse, if one takes into account the distance between these two devices with an appropriate electrical circuit (see fig. 7).

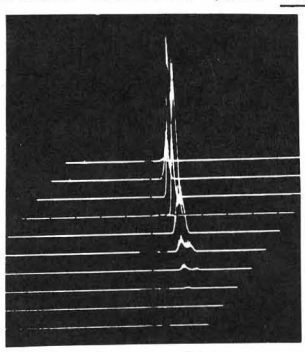

Fig. 7: Phase ellipse measured with slit and profile monitor

To make a precise but slow emittance measurement we use two corresponding slits, e.g. FN1 and FN3. Both slits have small openings and the transmitted intensity on the beam stopper BN4 is recorded. At first we move one slit stepwise across the beam and the other one scans it at each step. Then we change the role of the slits and repeat. We show in fig. 8 three dimensions of the phase space at the slit FN1 and the planes along which we project the phase ellipsoid into the (x_1, x_1')-plane. We may write the displacement of a particle at slit FN3 as

$$x_3 = x_1 + \ell_{13} x_1' \qquad (1)$$

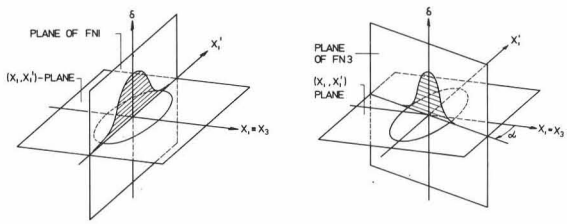

Fig. 8: The precise emittance measurement. The projection of the phase ellipsoid and a measured signal are sketched.

where x_1 is the distance, x_1' the slope of the particle at slit FN1 and ℓ_{13} the distance between the two slits. From this we get the angle α to

$$\tan\alpha = -\ell_{13} \qquad (2)$$

In the horizontal plane the measured projection of the phase ellipsoid depends upon the energy width and on the dispersion path of the incoming beam. The phase area in the vertical plane is independent of the dispersion path if the phase ellipsoid is upright along the momentum axis. In table 1 we show, for a comparison, the results of an emittance measured by these different methods.

Table 1: A comparison between different emittance measuring methods (5 % intensity level).

Measuring method	Emittance in (mm•mrad)ε/π		
	Horizont.	Vertic.	Error
Fast with two MNP-s	11.9	16.3	< 30%
Fast with two FN-s	9.6	10.8	25%
Slow with two FN-s	12.4	15.6	< 10%

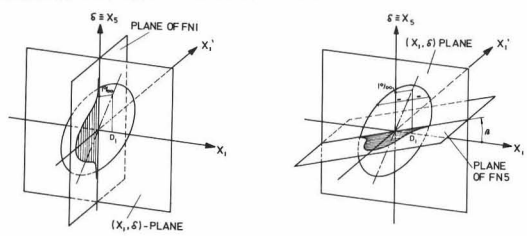

Fig. 9: Measurement of D_1. The projection of the phase ellipsoid, a measured signal and the evaluation of D_1 are shown.

6.1.2 In general, the horizontal dispersion path has a non vanishing displacement D_1 and a slope D_1' with respect to the optical axis at the slit FN1. To measure these parameters of the beam we make use of the slits FN1, FN3 and FN5, while recording the inten-

sity on BN4. Behind the analysing system at FN5 we get a dispersive image of the source at FN1. The displacement of a particle at the image may be written as follows

$$x_5 = M_{11}x_1 + M_{16}\delta \qquad (3)$$

where M_{11} is the magnification, M_{16} the dispersion of the analysing system and δ is the momentum deviation of the particle from the mean momentum. The projection of the beam along the FN1 and FN5 planes into the (x_1, δ)-plane is shown in fig.9. We use these two slits in the same manner as already described in 6.1.1. The angle β is given by equation (3):

$$\mathrm{tg}\beta = M_{11}/M_{16} \qquad (4)$$

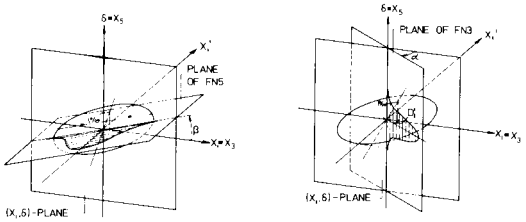

Fig. 10: Measurement of D_1'. The projection of the phase ellipsoid, a measured signal and the evaluation of D_1' are shown.

From this measurement we get D_1 as shown in fig. 9.
To get information about the slope, D_1' of the dispersion path we scan the beam with the slits FN3 and FN5. In fig. 10 we show the planes of these slits, transformed back to FN1. By measuring the intensity in these planes we project the phase ellipsoid into the (x_1, δ)-plane. This measurement is meaningful, only if, for any value of δ in the whole momentum range,

$$(x_1)_m < \ell_{13} \cdot (x_1')_m \qquad (5)$$

where the subscript m means the maximum value. To show how the displacement x_5 is related to the displacement x_3 and to x_1' and δ we first transform the slit FN3 back to the slit FN1, and then forward to the slit FN5. We then get

$$x_5 = M_{11}(x_3 - \ell_{13}x_1') + M_{16}\delta \qquad (6)$$

If the expression (5) holds, i.e. we have a small waist at FN1, we may calculate D_1', as indicated in fig. 10. In table 2 we listed the results of some beam quality measurements.

Table 2: Data of the incoming beam (5 % intensity level).

Date	Hor.Emitt. mm•mrad	Ver.Emitt. mm•mrad	D_1 mm	D_1' mrad	δ %
19.4.74	π•(10±1.)	—	-.4±.1	2±.5	.8±.1
4.3.75	π•(15±2)	—	2.2±.1	.5±.2	1.2±.1
7.7.75	π•(10±1)	—	0. ±.1	-.3±.2	1.1±.1
1.8.75	π•(12±1.2)	π•(16±1.5)	.1±.1	-.5±.2	1.3±.1

6.2 Injected beam. As has been shown[6], one can calculate the emittance of the beam in an accelerator in both planes if the betatron frequency is known and the beam diameter over some turns has been measured. Such a measurement also shows how well the beam has been matched to the acceptance of the accelerator. To get this information we use the three ΣΔR-probes[7] and two profile monitors in the radial plane of the ring accelerator. The profile monitor displays the radial intensity distribution of the first 5-6 turns. In fig. 11 we see an example of a matched beam. For measuring the emittance in the vertical plane we have only one profile monitor. This is not sufficient to decide whether the beam is properly matched in that plane. Further information can be gained by plotting the intensity distribution on the three fingers of the ΣΔR-probes separately, and using the "profile turbine". At the slit FN5 we know from the measurements on the incoming beam (described in 6.1.2) the relationship between displacement x_5 and momentum deviation δ. Then, to examine the energy matching of the beam in the accelerator, we use a small opening in the slit FN5 to select a momentum and measure the radial distribution of the beam (see fig. 12).Doing this for different momenta we may determine the dependence of the displacement and slope of the beam on the momentum.

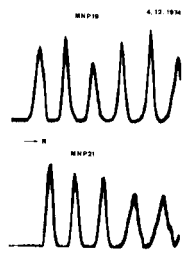

Fig. 11: First turns of a matched beam measured with two profile monitors.

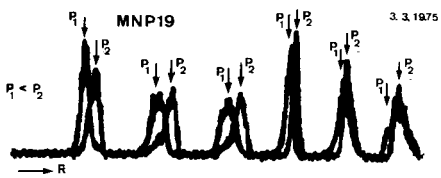

Fig. 12: Measurement of the energy matching with a profile monitor.

7. Future prospects

As the results of our measurements on the incoming beam show, its quality is not very reproducible and in consequence we must retune the transfer line from time to time. To achieve faster tuning we must be able to adjust each parameter of the injected beam. This is not a trivial task especially for the parameters describing the energy matching. To find a solution for this problem, we invented a programme called GRTRN[8] which runs on the accelerators' control computer. To calculate the beam envelope along the

transfer line we use the actual excitation of the elements and the measured incoming beam parameters. As figure 2 shows we have quite enough information on the beam size along the transfer line. Our next goal is to establish a better agreement between measurements and calculations. On this basis we hope to find a method for faster tuning.

References

[1]) J. Zichy, The injection path between the Philips Cyclotron and the ring accelerator SIN Report TM-06-12 (1970)

[2]) H.A. Enge, Report on Ion-optic Work on the SIN Beam Transfer System (1972)

[3]) L. Rezzonico, Thermische Untersuchungen an den Profilmonitorfingern SIN Report TM-09-30 (1972)

[4]) R. Reimann, Rückwirkungsfreie Intensitätsmessung an einem gepulsten Ionenstrahl Journal of Appl. Mathematics and Physics (ZAMP) Vol. 25 (1974)

[5]) L. Rezzonico, Elektronik für die Auswertung der Signale der Ionisationskammern SIN Report AN-09-28 (1973)

[6]) W. Joho, Beam transfer between accelerators, these Proceedings, p. 209

[7]) M. Olivo, Beam Diagnostic Equipment for Cyclotrons, these Proceedings, p. 331

[8]) J. Collins, Program Description of Graphic TRaNsport SIN Report (1974)

For further informations see the SIN"Tätigkeitsbericht" for the years 1972, 1973,1974.